



Lindbladian route towards thermalization of a Luttinger liquid


Ádám Bácsi ^{1,2,3,*} and Balázs Dóra ^{1,4}

¹*MTA-BME Lendület Topology and Correlation Research Group, Budapest University of Technology and Economics, Műgyetem rkp. 3., H-1111 Budapest, Hungary*

²*Department of Mathematics and Computational Sciences, Széchenyi István University, 9026 Győr, Hungary*

³*Jožef Stefan Institute, Jamova 39, Ljubljana SI-1000, Slovenia*

⁴*Department of Theoretical Physics, Institute of Physics, Budapest University of Technology and Economics, Műgyetem rkp. 3., H-1111 Budapest, Hungary*

 (Received 4 November 2022; revised 15 March 2023; accepted 16 March 2023; published 24 March 2023)

We study the nonequilibrium dynamics of a Luttinger liquid after a simultaneous quantum quench of the interaction and dissipative quench to the environment within the realm of the Lindblad equation. When the couplings to the environment satisfy detailed balance, the system is destined to thermalize, which we follow using bosonization. The thermodynamic entropy of the system, which also encodes information about the entanglement with the environment, either exhibits a maximum and minimum or grows monotonically before reaching its thermal value in a universal fashion. The single-particle density matrix reveals interesting features in the spatiotemporal “phase diagram,” including thermal, prethermal, and dissipation enhanced sudden quench Luttinger liquid behavior, as well as dissipation, enhanced Fermi liquid response.

DOI: [10.1103/PhysRevB.107.125149](https://doi.org/10.1103/PhysRevB.107.125149)

I. INTRODUCTION

Nonequilibrium dynamics and quantum quenches have attracted enormous attention ever since the manipulation of quantum systems became experimentally accessible in cold atomic gases [1–4]. In particular, sophisticated experimental methods enable the study of nonequilibrium dynamics in one-dimensional quantum systems [5,6]. These studies provide essential information about relaxation and equilibration, prethermalization and thermalization in a large variety of settings, incorporating topological and strongly interacting systems as well. Understanding nonequilibrium quantum dynamics is also essential for applications in quantum metrology [7], quantum computation and information processing [8].

Among the most fascinating topics, thermalization represents a central theme in nonequilibrium dynamics [9–11]. Closed quantum systems starting from a pure state do not thermalize due to unitary dynamics. However, a small subsystem can in principle thermalize since the rest of the system can act as an effective heat bath. This phenomenon is absent from integrable systems, where the large number of constants of motion prevents the subsystem from thermalization [12,13]. Nonintegrable systems, on the other hand, display subsystem thermalization [14], though these are rather hard to analyze [15] due to their nonintegrability.

Here we take a different approach to study thermalization and investigate open quantum systems. In particular, we focus on strongly interacting one-dimensional fermions, undergoing a sudden quantum quench [16–24] as well as dissipative coupling to environment [25,26]. The resulting open quantum

system thermalizes when couplings to environment satisfy detailed balance [25,27,28]. As a result, we are able to follow *exactly* the build up of Luttinger liquid (LL) physics and its competition with nonunitary dynamics due to environment and the eventual thermalization of the system.

We find the thermodynamic entropy of the system, which quantifies the entanglement with environment, can follow two qualitatively distinct time evolutions, depending on the environment temperature and interaction strength. It either exhibits a maximum, then a minimum or grows monotonically before reaching the thermal value. We argue that these features are typical in thermalizing open quantum systems. The single-particle density matrix reveals a whole zoo of strongly correlated features, such as dissipation enhanced sudden quench LL and Fermi liquid behavior, thermal, and prethermal LL. Due to the generality and universality of the LL picture, our approach applies to a great variety of low-dimensional fermionic, bosonic, and spin systems.

II. THERMALIZING LUTTINGER LIQUID

We study the low-energy behavior of a one-dimensional fermionic system, forming a Luttinger liquid [29]. The system is prepared in the ground state of a noninteracting Fermi gas, and the fermionic interaction is switched on suddenly at $t = 0$. Upon bosonization, the time-dependent Hamiltonian is

$$H = \sum_{q>0} [\omega(q, t)(b_q^+ b_q + b_{-q}^+ b_{-q}) + g(q, t)(b_q b_{-q} + b_q^+ b_{-q}^+)], \quad (1)$$

where the summation runs over all positive momenta. In the formula, $\omega(q, t) = v_F q + \Theta(t)g_4 q$ and $g(q, t) = \Theta(t)g_2 q$ with v_F the Fermi velocity and g_2 and g_4 describing the

*bacs.adam@sze.hu

forward scattering induced by the interaction between fermions of opposite and same chiralities, respectively [29]. For $t > 0$, the interacting Hamiltonian is diagonalized by a Bogoliubov transformation [29] as

$$H = E_0 + \sum_{q>0} cq(d_q^+ d_q + d_{-q}^+ d_{-q}), \quad (2)$$

where $c = \sqrt{(v_F + g_4)^2 - g_2^2}$ is the renormalized sound velocity and $E_0 = \sum_{q>0} (c - v_F - g_4)q$ is the ground-state energy. The sudden quantum quench described in Eq. (1) has been extensively investigated in previous studies [18,30,31].

In addition to sudden quantum quench, we also couple the system to environment at $t = 0$, therefore dissipative processes are also taken into account during the time evolution. For simplicity, we use the Lindblad equation [25] for the density matrix as $\partial_t \rho = -i[H, \rho] + \mathcal{D}[\rho]$ where the dissipation reads as

$$\mathcal{D}[\rho] = \sum_q \gamma |q\rangle [(n(T, q) + 1) \mathcal{D}_{\downarrow, q}[\rho] + n(T, q) \mathcal{D}_{\uparrow, q}[\rho]] \quad (3)$$

involving $\mathcal{D}_{\downarrow, q}[\rho] = d_q \rho d_q^+ - \frac{1}{2} \{d_q^+ d_q, \rho\}$ and $\mathcal{D}_{\uparrow, q}[\rho] = d_q^+ \rho d_q - \frac{1}{2} \{d_q d_q^+, \rho\}$. This approach remains meaningful in the weak coupling, $\gamma \ll c$ limit. The processes described by the jump operators [25,26,32] d_q in \mathcal{D}_{\downarrow} and d_q^+ in \mathcal{D}_{\uparrow} are responsible for annihilating and creating bosonic quasiparticles, respectively. Qualitatively similar results are expected for various combinations of these jump operators. In the fermionic language, these involve energy exchange with the environment and describe a mixture of relaxation and excitation of fermions with momentum q , as discussed in Ref. [33]. The prefactors of dissipators include the Bose-Einstein distribution, $n(T, q) = (e^{c|q|/T} - 1)^{-1}$ with T the temperature, ensuring that the dissipative dynamics obeys detailed balance [27,34]. Note that the jump processes considered in Eq. (3) are one of the many possible choices to model detailed balance [25,35,36]. More complicated jump processes between different momentum states could also be taken into account. In this work, however, we focus on the simplest but physically still relevant dissipation.

Based on the Lindbladian dynamics, the time dependence of the following expectation values, which play crucial role in most physical quantities as we shall see later, are obtained analytically as

$$n_q(t) = \text{Tr}[\rho(t) d_q^+ d_q] = n(T, q) + (n_0 - n(T, q)) e^{-\gamma q t}, \quad (4a)$$

$$m_q(t) = \text{Tr}[\rho(t) d_q^+ d_{-q}^+] = m_0 e^{(2ic - \gamma)|q|t}, \quad (4b)$$

where the initial values are $n_0 = (1 - K)^2 / (4K)$ and $m_0 = (1 - K^2) / (4K)$ with $K = \sqrt{(v_F + g_4 - g_2) / (v_F + g_4 + g_2)}$ the LL parameter. Note that $K > 1$ and $K < 1$ correspond to attractive and repulsive interaction, respectively. Furthermore, $n_q(t)$ is invariant under $K \leftrightarrow 1/K$ while $m_q(t)$ changes sign. This symmetry ensures that the our results in the present paper remain also invariant for $K \leftrightarrow 1/K$, hence we focus on repulsive interactions ($K < 1$) only.

III. ENTROPY

To follow the thermalization dynamics, we investigate the time-dependence of the von Neumann entropy, defined as $S(t) = \text{Tr}[\rho(t) \ln \rho(t)]$. Initially, the system is in the (pure) ground state of the noninteracting Hamiltonian and, hence, $S(0) = 0$. On general ground, we expect two distinct type of time dependencies. Qualitatively, after the sudden quantum quench, a significant number of excitation are created, contributing to an initial sharp increase of the entropy. When the final temperature is small, these excitations need to be extracted from the system by the dissipative process, thus after a maximum, the entropy should decrease. As we show below, after reaching a minimum, the entropy increases to its steady state value. On the other hand, for large final temperatures, even more excitations are present in the thermal state than those created by the sudden quantum quench, therefore the entropy is expected to continue its initial increase monotonically throughout the time dependence.

The full time dependent entropy is evaluated from

$$S(t) = 2 \sum_{q>0} [(N_q(t) + 1) \ln(N_q(t) + 1) - N_q(t) \ln N_q(t)], \quad (5)$$

where

$$N_q(t) = \sqrt{\left(n_q(t) + \frac{1}{2}\right)^2 - |m_q(t)|^2} - \frac{1}{2}. \quad (6)$$

The derivation of Eq. (5) can be found in Supplementary Material of Ref. [37]. The behavior of the entropy is best understood by inspecting the time dependence of $N_q(t)$ for several wave numbers (see Appendix). For large q , when $q > 2\ell_T^{-1} \ln |(1 + K)/(1 - K)|$ with the thermal length $\ell_T = c/T$, the initial ramp up period, corresponding to generating bosons, ends at a maximum value and the $N_q(t)$ decreases to its steady value which is set by the Bose-Einstein distribution $n(T, q)$. This feature is a consequence of that the quantum quench generates more bosons than the expected value in thermal equilibrium and, hence, the dissipative coupling to environment extracts the surplus of bosons from the system and causes thermalization. For small wave numbers, however, the thermal equilibrium value of bosons is large since $n(T, q) \sim T/q$ and, therefore, the number of bosons keeps increasing during thermalization after the initial boson generation.

The time evolution of the entropy is shown in Fig. 1 for several values of the temperature using the conventional momentum space cutoff [29] as $\exp(-\alpha|q|)$ with α the short distance cutoff. Note that c/α is the high energy scale which very often plays the role of the bandwidth [38]. Initially, the entropy grows as $t \ln(t)$ and exhibits two distinct typical behaviors for longer times, depending on the environmental temperature, as discussed above.

At low temperature, the entropy first reaches a maximum and then decreases due to the extraction of bosons out of the higher momentum modes. This decaying regime ends at a minimum and the steady value of the entropy, $S_{th}(T) = L\pi T/3c$, which is the thermal entropy, is approached in a

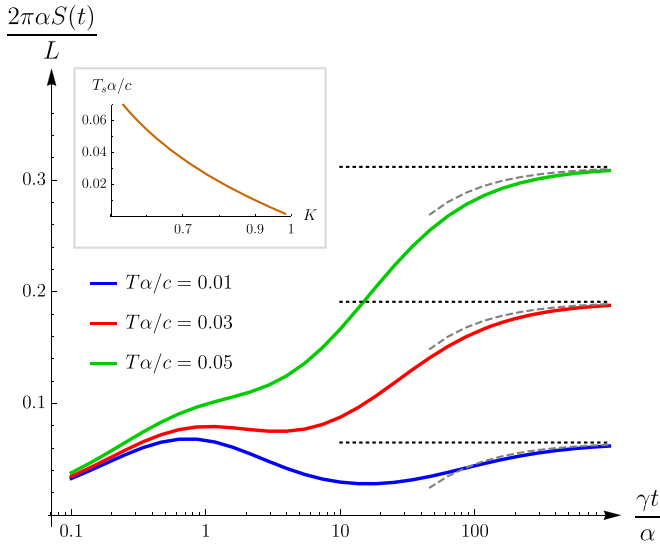


FIG. 1. The time evolution of the entropy at several temperatures and $K = 0.7$. The black dotted line indicates the steady, thermal value. The gray, dashed lines exhibit Eq. (7) describing the late time behavior of the entropy. (Inset) K dependence of the temperature T_s separating the two characteristics of the entropy evolution.

universal fashion as

$$S(t) = S_{th}(T) - \frac{L}{\pi\gamma t}, \quad (7)$$

which is valid for $\gamma t \gg \ell_T$. At zero temperature, however, this condition can never be fulfilled and, in this special case, the entropy decreases all the way to its thermal value which is zero. On the other hand, at high temperatures, the entropy increases monotonically and also reaches its thermal value as in Eq. (7). This feature is the consequence of the short thermal length which dictates monotonically increasing number of bosons for most wave numbers.

The two characteristic time evolutions are separated by the temperature T_s which depends only on K as shown in the inset of Fig. 1, but is independent of γ/c and α for $\alpha \ll \ell_T$ [39]. This universal feature is a consequence of the interplay between the initial boson generation by the quantum quench and the thermalization driven by the coupling to the environment. Similar behavior can be observed in the time evolution of other thermodynamic quantities, such as the Rényi entropy or total energy (see Appendix).

Finally, let us make a remark on the characteristic timescales emerging in the time evolution of the entropy. These are $\tau_\alpha = \alpha/\gamma$ and $\tau_T = \ell_T/\gamma$. The former corresponds to the inverse of the typical energy scale related to dissipation [37], $\Gamma \sim \gamma/\alpha$ as was found when comparing bosonization to dissipative lattice models. The latter follows from the comparison of the dimensionless dissipative timescale, Γt and the dimensionless thermal scale, $c/(\alpha T)$.

At low temperatures, the timescales obey $\tau_\alpha \ll \tau_T$ (i.e., the temperature is much smaller than the bandwidth) and, as a consequence, the thermalization of the entropy exhibits two separate stages. At high temperatures, however, the two timescales are less distinguishable, leading to a monotonous increase of the entropy.

IV. SINGLE-PARTICLE DENSITY MATRIX

Correlation functions display more complex behavior than the entropy. To gain insight into the time evolution of spatial correlations, we study the equal-time single-particle density matrix. Using the fermionic field operator $\Psi_R(x)$ [29], the single-particle density matrix is defined as $G(x, t) = \text{Tr}[\rho(t)\Psi_R(x)\Psi_R^\dagger(0)]$, yielding [33]

$$G(x, t) = G_0(x) \exp\left(-\sum_{q>0} \frac{4\pi}{Lq} (1 - \cos(qx)) n_q^b(t)\right). \quad (8)$$

where $G_0(x) = 1/(2\pi(x + i\alpha))$ is the initial correlation function obeying the well-known $1/x$ decay of free fermionic correlations [29]. The expectation value of noninteracting b bosons, $n_q^b(t) = \text{Tr}[\rho(t)b_q^\dagger b_q]$, is

$$n_q^b(t) = \frac{(1-K)^2}{4K} + \frac{K^2+1}{2K} n_q(t) + \frac{K^2-1}{2K} \text{Re}(m_q(t)). \quad (9)$$

From these, the spatiotemporal dependence of the single-particle density matrix is calculated exactly, as detailed in Appendix. Since the resulting expression is not too illuminating, we focus on its behavior in various limits of interest. We also work in the scaling limit, when $|x|$, $2ct$ and ℓ_T (and their combinations) are all much larger than α . However, in order to make contact with the nondissipative sudden quantum quench results [18,30,31], we allow for γt to be comparable to α . As already advertised, we use the weak coupling for the Lindblad equation, $c \gg \gamma$.

We start by investigating the steady state, when thermalization occurs. From the steady value of

$$n_q^b(\infty) = \frac{(1-K)^2}{4K} + \frac{K^2+1}{2K} n(T, q), \quad (10)$$

we obtain the characteristic thermal LL behavior [29,40] as

$$G^{LL}(x, \infty) = \frac{1}{2\pi\alpha} \begin{cases} \left(\frac{\alpha}{x}\right)^{(K+K^{-1})/2}, & x \ll \ell_T, \\ \left(\frac{2\pi\alpha}{\ell_T}\right)^{\frac{K+K^{-1}}{2}} e^{-\frac{\pi(K+K^{-1})}{2} \frac{x}{\ell_T}}, & \ell_T \ll x, \end{cases} \quad (11)$$

which remains also valid for the region $x \ll \gamma t$. For distances shorter than the thermal length, it follows the characteristic power-law decay with the conventional LL exponent. For long distances, exponential decay is found as expected in thermal equilibrium [29].

We now focus on the early stage of time evolution, i.e., when $\alpha + \gamma t \ll \ell_T$ but $\gamma t \ll x$, and find

$$\frac{G(x, t)}{G_0(x)} = \left(\frac{\alpha}{\min(x, 2ct)}\right)^{-\frac{(K-K^{-1})^2}{2}} \left(1 + \frac{\gamma t}{\alpha}\right)^{\frac{(1-K)^2(K^2+1)}{4K^2}}. \quad (12)$$

The first term represents the conventional sudden quench result [18,31], while the second one is responsible for a *dissipation induced enhancement* factor, which is always bigger than 1. This enhancement is understood by realizing that after a nondissipative quantum quench, correlations start to propagate along light cones [41] and suppress the single-particle density matrix [i.e., the first term in Eq. (12)]. However, this propagation is slowed down significantly due to the quantum

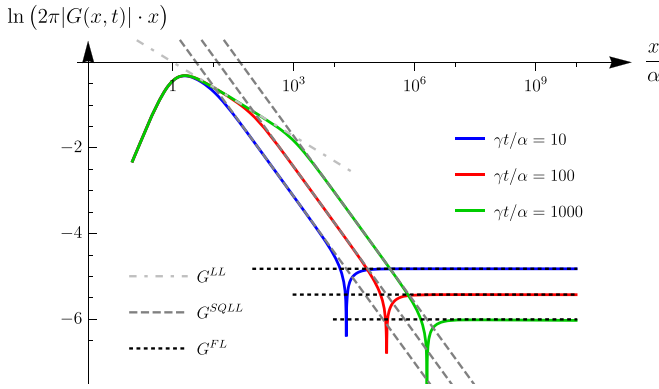


FIG. 2. Spatial decay of the single-particle density matrix at several time instants in the early stage of time evolution for $\gamma t \ll \ell_T$ with $K = 0.5$, $c/\gamma = 10^3$, and $\alpha/\ell_T = 10^{-5}$. The three characteristic behaviors, namely, thermal LL, dissipation enhanced sudden quench LL and dissipation enhanced Fermi liquid behaviors are clearly visible with increasing x .

Zeno effect induced by the continuously coupling to environment. As a result, the suppression of correlation by the sudden quench is not as effective as without the dissipative environment, therefore an additional enhancement factor due to dissipation appears.

It is illuminating to further analyze Eq. (12) in limiting cases. For $\alpha + \gamma t \ll 2ct \ll x$, the single-particle density matrix displays dissipation enhanced Fermi liquid behavior, namely, it retains its initial spatial decay as $G^{FL}(x, t) = G_0(x)Z(t) \sim Z(t)/x$, characteristic to a Fermi liquid with time dependent Landau's quasiparticle weight [18] as

$$Z(t) = \left(\frac{2ct}{\alpha}\right)^{-\left(\frac{K-K^{-1}}{2}\right)^2} \left(1 + \frac{\gamma t}{\alpha}\right)^{\frac{(1-K)^2(1+K^2)}{4K^2}}. \quad (13)$$

In the absence of dissipation ($\gamma = 0$), we recover previous results [18,31] as $Z(t) \sim t^{-((K-K^{-1})/2)^2}$. In the presence of dissipation, on the other hand, the temporal decay in the quasiparticle weight is less pronounced due to the dissipation induced enhancement factor as $Z(t) \sim t^{-(1-K)^2/(2K)}$. The absolute value of this second exponent in $Z(t)$ for $\gamma > 0$ is always smaller than the one corresponding to $\gamma = 0$.

For $\alpha + \gamma t \ll x \ll 2ct$, we find dissipation enhanced sudden quench LL behavior from Eq. (12) as

$$G^{SOLL}(x, t) = \frac{1}{2\pi\alpha} \left(\frac{\alpha}{x}\right)^{\left(\frac{K+K^{-1}}{2}\right)^2} \left(1 + \frac{\gamma t}{\alpha}\right)^{\frac{(1-K)^2(K^2+1)}{4K^2}}, \quad (14)$$

describing the same spatial decay as found for a sudden quantum quench in Ref. [31], featuring the sudden quench LL exponent. The correlations are also enhanced in time by dissipation in this regime. The spatial decay of the single-particle density matrix for early times is shown in Fig. 2, reflecting the presence of the limiting cases.

For the late time evolution with $\ell_T \ll \gamma t \ll x$, we find peculiar behavior what we coin as prethermal LL response as

$$G^{\text{preth}}(x, t) = \frac{1}{2\pi\ell_T} \left(\frac{\gamma t}{xe}\right)^{(K+K^{-1})\frac{\gamma t}{\ell_T}}, \quad (15)$$

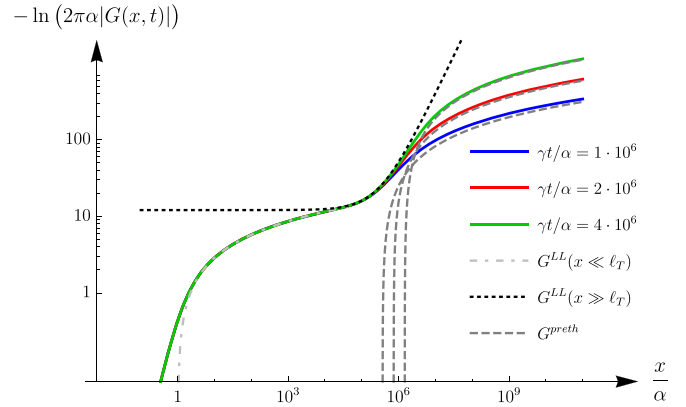


FIG. 3. Spatial decay of the single-particle density matrix at several time instants for late times, $\gamma t \gg \ell_T$ with $K = 0.5$, $c/\gamma = 10^3$, and $\alpha/\ell_T = 10^{-5}$. The three main characteristics, namely, power-law decay within the thermal correlation length, thermal exponential decay above the thermal correlation length and prethermal LL behavior are identified with increasing x .

following a special power-law spatial decay with a time-dependent exponent as well as exponential temporal decay. However, the exponent itself can be arbitrarily large, and causes a very rapid suppression of correlations [42]. In the prethermal phase, the physical quantities we investigated do not exhibit a plateau which is very often associated with prethermalization [10]. In our framework, the prethermal phase features a time evolution which essentially differs from the relaxation of the Fermi liquid and also from the actual thermalization which is observed when γt becomes comparable with or larger than x .

In the $x \ll \gamma t$ region, the steady state behavior is dominated by the thermal LL physics from Eq. (11). The features of late time behavior can be recognized in Fig. 3.

Based on these results, we can construct the spatiotemporal map or “phase diagram” of the single-particle density matrix, revealing the various regions induced by the intricate interplay of unitary and nonunitary dynamics from sudden quantum quench and dissipation quench, respectively. This is shown in Fig. 4. Finally, we mention that in the absence of dissipation ($\gamma = 0$), the line of $x = \gamma t$ is tilted to zero and vanishes from the map, together with $\ell_T \rightarrow \infty$. Consequently, we are only left with the regions of the Fermi liquid behavior and the sudden quench LL behavior (SOLL) without the dissipation induced enhancement.

V. SUMMARY

We study thermalization and the interplay of unitary and nonunitary dynamics on an interacting one-dimensional system, a Luttinger liquid. By using a Lindblad equation description with couplings to environment satisfying detailed balance, thermalization is guaranteed in the long time limit. Before reaching it, the von Neumann entropy of the system, which quantifies the amount of entanglement with the environment, either displays a maximum and minimum during the time evolution or grows monotonically before hitting its thermal value. These features are expected to be generic for a wide range of systems when undergoing simultaneous quantum and

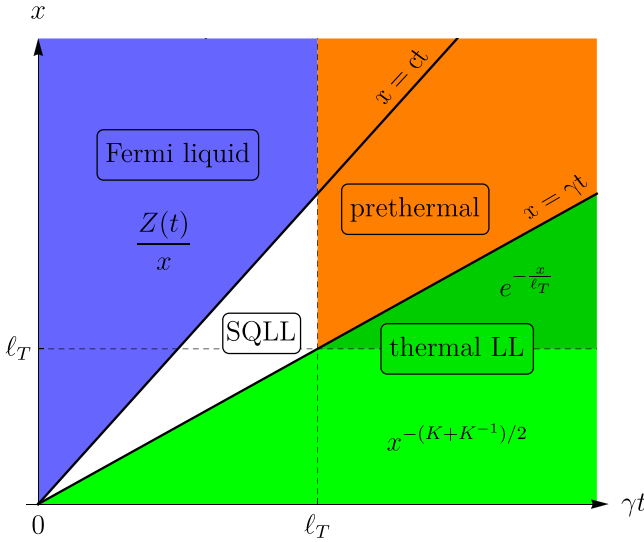


FIG. 4. The spatiotemporal map or “phase diagram” of the single-particle density matrix, displaying the various behaviors such as dissipation enhanced sudden quench LL, dissipation enhanced Fermi liquid, prethermal, and thermal LL. The dominant timescales are the same as for the time evolution of the entropy.

environmental quench since these are direct consequences of the initial creation of excitations and the subsequent dissipative dynamics.

Correlation functions exhibit even more complex behavior, what we demonstrate by focusing on the fermionic single-particle density matrix. We find that the presence of dissipation can enhance sudden quench correlations through the dissipation induced Zeno dynamics. We identify several distinct behaviors during the space-time evolution corresponding to thermal, prethermal and dissipation enhanced sudden quench Luttinger liquid behavior as well as dissipation enhanced Fermi liquid response.

ACKNOWLEDGMENTS

This research was supported by the Ministry of Culture and Innovation and the National Research, Development and Innovation Office within the Quantum Information National Laboratory of Hungary (Grant No. 2022-2.1.1-NL-2022-00004) K134437, K142179 and by a grant of the Ministry of Research, Innovation and Digitization, CNCS/CCCDI-UEFISCDI, under projects number PN-III-P4-ID-PCE-2020-0277. Á.B. acknowledges the support of the Slovenian Research Agency (ARRS) under J1-3008.

APPENDIX A: TIME EVOLUTION OF THE TOTAL ENERGY AND RÉNYI ENTROPY

Similarly to the entropy presented in the main text, other thermodynamic quantities also feature two different time-dependence depending on the temperature of the thermalizing environment. In this appendix, we demonstrate the time evolution of the total energy and the Rényi entropy. The latter is

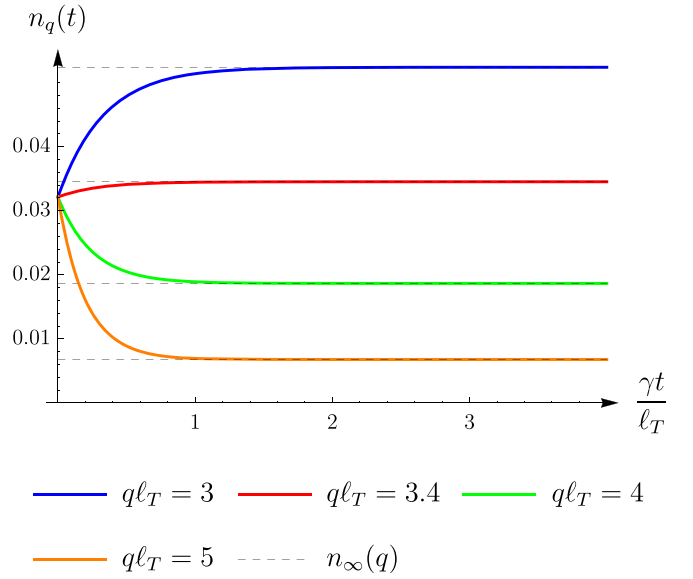


FIG. 5. Time dependence of $n_q(t)$ at different wave numbers. The function starts at $n_0(K) = (1 - K)^2/(4K)$ in each wave-number channel and then monotonously tends to the thermal value, $n(T, q)$.

defined as $E(t) = \text{Tr}[\rho(t)H]$ with H the Hamiltonian of the interacting system.

The total energy is evaluated as

$$E(t) = E_0 + 2 \sum_{q>0} cq n_q(t), \quad (\text{A1})$$

where $E_0 = \sum_{q>0}(c - v_F - g_4)q$ is the interacting ground-state energy. The time dependence occurs through the quantity of $n_q(t)$ defined in Eq. (4a) of the main text, respectively. Figure 5 shows that $n_q(t)$ starts at the same initial value, $n_0 = (1 - K)^2/4K$ and approaches exponentially the steady value, $n(T, q)$.

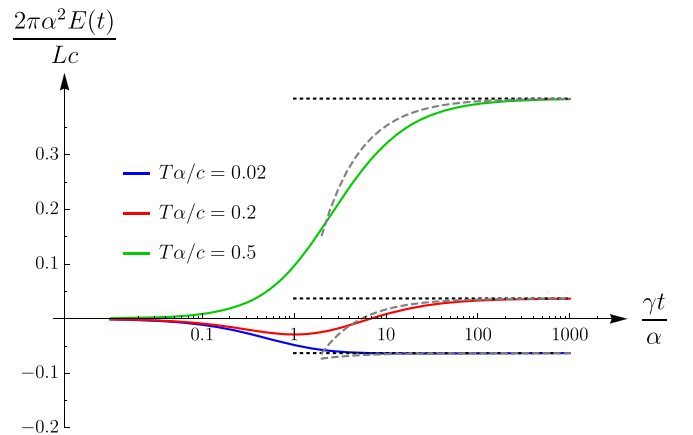


FIG. 6. The time evolution of total energy at several temperature values. The black dotted lines indicate the steady value of the energy, (A4). The gray dashed lines show the long time behavior, (A3). For the plot, $K = 0.7$ is set.

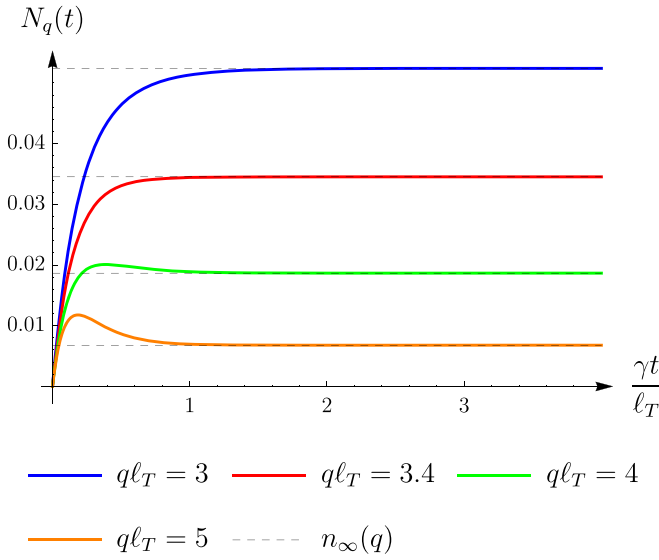


FIG. 7. Time dependence of $N_q(t)$ at different wave numbers. At high wave numbers, $N_q(t)$ exhibits a maximum and decreases back to its thermal value, $n(T, q)$. At low wave numbers, the function increases monotonously. Furthermore, it is remarkable that high momentum modes thermalize faster than low energy modes.

Substituting (4a) into (A1), the integral over q yields

$$E(t) = \frac{Lc}{2\pi\alpha^2} \left[-\frac{(1+K)^2}{2K} \frac{\gamma t(2\alpha + \gamma t)}{(\alpha + \gamma t)^2} + 2 \left(\frac{\alpha}{\ell_T} \right)^2 \left(\Psi_1 \left(\frac{\alpha + \gamma t}{\ell_T} \right) - \Psi_1 \left(\frac{\alpha}{\ell_T} \right) \right) \right] \quad (\text{A2})$$

with $\Psi_1(y)$ the polygamma function. The long-time behavior of the total energy is obtained as

$$E(t) = E_{th}(T) - \frac{Lc}{2\pi\ell_T\gamma t} \quad (\text{A3})$$

with the steady state thermal value

$$E_{th}(T) = -\frac{Lc}{2\pi\alpha^2} \left(\frac{(1+K)^2}{2K} + 2 \left(\frac{\alpha}{\ell_T} \right)^2 \Psi_1 \left(\frac{\alpha}{\ell_T} \right) \right). \quad (\text{A4})$$

The complete time evolution is shown in Fig. 6. It can be seen that at high temperatures, the total energy monotonously increases, indicating that the initially generated amount of bosons is less than that of the thermal state. At low temperatures, however, an initial reduction can be observed due to the extraction of bosons on the high momentum (high energy) modes. Later, the energy increases back when high energy modes are already thermalized and only low energy modes exhibit dynamics.

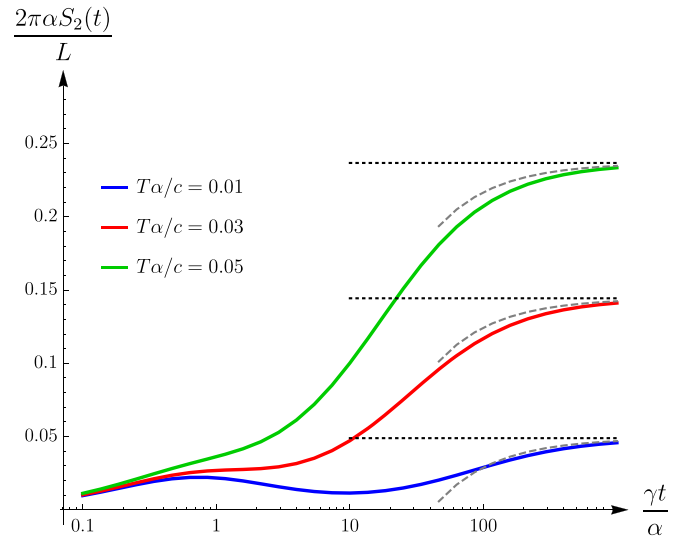


FIG. 8. The time evolution of the Rényi entropy at several temperature values. The black dotted lines indicate the steady state thermal value, $S_{2,T}$. The gray dashed lines show the long time behavior which is analytically obtained as $S_2(t) = S_{2,T} - L/(\pi\gamma t)$. For the plot, $K = 0.7$ is set.

Among thermodynamic quantities, the Rényi-2 entropy plays an important role because of its experimental accessibility [43,44]. The Rényi entropy is defined as $S_2(t) = -\ln \text{Tr}[\rho(t)^2]$ and is calculated as

$$S_2(t) = 2 \sum_{q>0} \ln(2N_q(t) + 1) \quad (\text{A5})$$

with $N_q(t)$ defined below Eq. (5). Figure 7 shows that in the low momentum (low energy) channels, $N_q(t)$ increases to its thermal value monotonously while at high q , the function has a maximum after which it decreases to the thermal value.

The Rényi entropy is computed numerically and the typical time evolution scenarios are shown in Fig. 8. At high temperatures, the entropy increases monotonically while at low temperatures, the initial growth of the entropy is followed by a decreasing period.

To summarize, similarly to the von Neumann entropy presented in the main text, both the total energy and the Rényi entropy exhibit two characteristic time evolution. These features can be explained by the interplay between the quantum quench and the dissipative dynamics. The quantum quench generates bosons in each momentum channels. For low momenta, this amount of boson is still less than it should be at thermal equilibrium and, hence, the dissipative dynamics will further increase the amount of bosons. For higher momentum, the quench-generated is already more than it should be in equilibrium and, therefore, dissipation extracts the surplus. By changing the temperature, the boarder between low and high momentum regimes are shifted resulting in temperature dependent characteristics in thermodynamic quantities.

APPENDIX B: ANALYTIC DERIVATION OF THE EQUAL-TIME SINGLE-PARTICLE DENSITY MATRIX

As presented in the main text, the single-particle density matrix is obtained as

$$G(x, t) = G_0(x) \exp \left(- \sum_{q>0} \frac{4\pi}{Lq} (1 - \cos(qx)) n_q^b(t) \right), \quad (\text{B1})$$

where $G_0(x)$ is the initial Green's function and $n_q^b(t)$ is the average number of b -bosons calculated in Eq. (9) of the main text. We substitute (9) into (B1) and take the thermodynamic limit leading to a q -integral instead of the sum. To regularize the integral, we use an exponential cutoff, $\sum_{q>0} \rightarrow \frac{L}{2\pi} \int_0^\infty dq e^{-\alpha|q|}$. The integral is carried out as

$$\begin{aligned} \ln \left(\frac{G(x, t)}{G_0(x)} \right) &= \frac{K^2 + 1}{2K} \left[\ln \left(\frac{\Gamma \left(1 + \frac{\alpha + \gamma t}{\ell_T} \right)^2}{\Gamma \left(1 + \frac{\alpha + \gamma t + ix}{\ell_T} \right) \Gamma \left(1 + \frac{\alpha + \gamma t - ix}{\ell_T} \right)} \right) - \ln \left(\frac{\Gamma \left(1 + \frac{\alpha}{\ell_T} \right)^2}{\Gamma \left(1 + \frac{\alpha + ix}{\ell_T} \right) \Gamma \left(1 + \frac{\alpha - ix}{\ell_T} \right)} \right) \right] \\ &+ \frac{(1 - K^2)^2}{16K^2} \ln \left(\frac{((\alpha + \gamma t)^2 + (x - 2ct)^2)((\alpha + \gamma t)^2 + (x + 2ct)^2)}{((\alpha + \gamma t)^2 + (2ct)^2)^2} \right) \\ &- \frac{(K^2 + 1)(1 - K)^2}{8K^2} \ln \left(1 + \frac{x^2}{(\alpha + \gamma t)^2} \right) - \frac{(1 - K)^2}{4K} \ln \left(1 + \left(\frac{x}{\alpha} \right)^2 \right), \end{aligned} \quad (\text{B2})$$

where $\Gamma(y)$ is the Gamma function.

-
- [1] A. Polkovnikov, K. Sengupta, A. Silva, and M. Vengalattore, Colloquium: Nonequilibrium dynamics of closed interacting quantum systems, *Rev. Mod. Phys.* **83**, 863 (2011).
- [2] I. Bloch, J. Dalibard, and W. Zwerger, Many-body physics with ultracold gases, *Rev. Mod. Phys.* **80**, 885 (2008).
- [3] J. Dziarmaga, Dynamics of a quantum phase transition and relaxation to a steady state, *Adv. Phys.* **59**, 1063 (2010).
- [4] M. A. Cazalilla, R. Citro, T. Giamarchi, E. Orignac, and M. Rigol, One dimensional bosons: From condensed matter systems to ultracold gases, *Rev. Mod. Phys.* **83**, 1405 (2011).
- [5] S. Erne, R. Bückler, T. Gasenzer, J. Berges, and J. Schmiedmayer, Universal dynamics in an isolated one-dimensional Bose gas far from equilibrium, *Nature (London)* **563**, 225 (2018).
- [6] M. Gring, M. Kuhnert, T. Langen, T. Kitagawa, B. Rauer, M. Schreitl, I. Mazets, D. A. Smith, E. Demler, and J. Schmiedmayer, Relaxation and prethermalization in an isolated quantum system, *Science* **337**, 1318 (2012).
- [7] G. Tóth and I. Apellaniz, Quantum metrology from a quantum information science perspective, *J. Phys. A: Math. Theor.* **47** (42), 424006 (2014).
- [8] M. Nielsen and I. Chuang, *Quantum Computation and Quantum Information* (Cambridge University Press, Cambridge, 2000).
- [9] T. Kinoshita, T. Wenger, and D. S. Weiss, A quantum Newton's cradle, *Nature (London)* **440**, 900 (2006).
- [10] T. Mori, T. N. Ikeda, E. Kaminishi, and M. Ueda, Thermalization and prethermalization in isolated quantum systems: a theoretical overview, *J. Phys. B: At. Mol. Opt. Phys.* **51**, 112001 (2018).
- [11] E. Kaminishi, T. Mori, T. N. Ikeda, and M. Ueda, Entanglement pre-thermalization in a one-dimensional Bose gas, *Nat. Phys.* **11**, 1050 (2015).
- [12] J. M. Deutsch, Quantum statistical mechanics in a closed system, *Phys. Rev. A* **43**, 2046 (1991).
- [13] M. Srednicki, Chaos and quantum thermalization, *Phys. Rev. E* **50**, 888 (1994).
- [14] M. Rigol, V. Dunjko, and M. Olshanii, Thermalization and its mechanism for generic isolated quantum systems, *Nature (London)* **452**, 854 (2008).
- [15] B. Bertini, F. H. L. Essler, S. Groha, and N. J. Robinson, Prethermalization and Thermalization in Models with Weak Integrability Breaking, *Phys. Rev. Lett.* **115**, 180601 (2015).
- [16] A. Widera, S. Trotzky, P. Cheinet, S. Fölling, F. Gerbier, I. Bloch, V. Gritsev, M. D. Lukin, and E. Demler, Quantum Spin Dynamics of Mode-Squeezed Luttinger Liquids in Two-Component Atomic Gases, *Phys. Rev. Lett.* **100**, 140401 (2008).
- [17] C. Karrasch, J. Rentrop, D. Schuricht, and V. Meden, Luttinger-Liquid Universality in the Time Evolution after an Interaction Quench, *Phys. Rev. Lett.* **109**, 126406 (2012).
- [18] M. A. Cazalilla, Effect of Suddenly Turning on Interactions in the Luttinger Model, *Phys. Rev. Lett.* **97**, 156403 (2006).
- [19] E. Perfetto and G. Stefanucci, On the thermalization of a Luttinger liquid after a sequence of sudden interaction quenches, *Europhys. Lett.* **95**, 10006 (2011).
- [20] D. B. Gutman, Y. Gefen, and A. D. Mirlin, Bosonization of one-dimensional fermions out of equilibrium, *Phys. Rev. B* **81**, 085436 (2010).
- [21] M. Buchhold, M. Heyl, and S. Diehl, Prethermalization and thermalization of a quenched interacting Luttinger liquid, *Phys. Rev. A* **94**, 013601 (2016).
- [22] P. Ruggiero, L. Foini, and T. Giamarchi, Large-scale thermalization, prethermalization, and impact of temperature in the quench dynamics of two unequal Luttinger liquids, *Phys. Rev. Res.* **3**, 013048 (2021).
- [23] E. Kaminishi, T. Mori, T. N. Ikeda, and M. Ueda, Entanglement prethermalization in the Tomonaga-Luttinger model, *Phys. Rev. A* **97**, 013622 (2018).

- [24] P. Moosavi, Emergence of generalized hydrodynamics in the non-local Luttinger model, *SciPost Phys.* **9**, 037 (2020).
- [25] H. Breuer and F. Petruccione, *The Theory of Open Quantum Systems* (Oxford University Press, 2002).
- [26] A. J. Daley, Quantum trajectories and open many-body quantum systems, *Adv. Phys.* **63**, 77 (2014).
- [27] A. Rajagopal, The principle of detailed balance and the Lindblad dissipative quantum dynamics, *Phys. Lett. A* **246**, 237 (1998).
- [28] Y. Ashida, K. Saito, and M. Ueda, Thermalization and Heating Dynamics in Open Generic Many-Body Systems, *Phys. Rev. Lett.* **121**, 170402 (2018).
- [29] T. Giamarchi, *Quantum Physics in One Dimension* (Oxford University Press, Oxford, 2004).
- [30] M. A. Cazalilla and M.-C. Chung, Quantum quenches in the Luttinger model and its close relatives, *J. Stat. Mech.* (2016) 064004.
- [31] A. Iucci and M. A. Cazalilla, Quantum quench dynamics of the Luttinger model, *Phys. Rev. A* **80**, 063619 (2009).
- [32] Y. Ashida, Z. Gong, and M. Ueda, Non-hermitian physics, *Adv. Phys.* **69**, 249 (2020).
- [33] A. Bácsi, C. P. Moca, and B. Dóra, Dissipation-Induced Luttinger Liquid Correlations in a One-Dimensional Fermi Gas, *Phys. Rev. Lett.* **124**, 136401 (2020).
- [34] Indeed, the ratio of the couplings of relaxation and excitation is $(1 + n(T, q))/n(T, q) = e^{c|q|/T}$.
- [35] I. Reichental, A. Klemmner, Y. Kafri, and D. Podolsky, Thermalization in open quantum systems, *Phys. Rev. B* **97**, 134301 (2018).
- [36] A. D'Abbruzzo and D. Rossini, Self-consistent microscopic derivation of Markovian master equations for open quadratic quantum systems, *Phys. Rev. A* **103**, 052209 (2021).
- [37] A. Bácsi, C. P. Moca, G. Zaránd, and B. Dóra, Vaporization Dynamics of a Dissipative Quantum Liquid, *Phys. Rev. Lett.* **125**, 266803 (2020).
- [38] Certain physical quantities, such as the particle density and ground-state energy, depend naturally on the bandwidth, while others, as we discuss below, are independent from it and are universal.
- [39] We note that qualitatively similar features are observed for other momentum space regularization schemes, e.g. sharp cutoff. The value of T_s may depend on the regularization but its existence and the presence of the two different characteristic time evolution seem to be universal.
- [40] M. A. Cazalilla, Bosonizing one-dimensional cold atomic gases, *J. Phys. B: At. Mol. Opt. Phys.* **37**, S1 (2004).
- [41] P. Calabrese and J. Cardy, Evolution of entanglement entropy in one-dimensional systems, *J. Stat. Mech.* (2005) P04010.
- [42] Eq. (15) is also multiplied by additional power-law terms as in Eq. (14), but the dominant decay stems from the time dependent exponent. Neglecting these power-laws is further justified in Fig. 3, where the exact expression from Eq. (8) is compared to Eq. (15).
- [43] R. Islam, R. Ma, P. M. Preiss, M. E. Tai, A. Lukin, M. Rispoli, and M. Greiner, Measuring entanglement entropy in a quantum many-body system, *Nature (London)* **528**, 77 (2015).
- [44] T. Brydges, A. Elben, P. Jurcevic, B. Vermersch, C. Maier, B. P. Lanyon, P. Zoller, R. Blatt, and C. F. Roos, Probing Rényi entanglement entropy via randomized measurements, *Science* **364** (6437), 260 (2019).